

FSI Analysis of the Coughing Mechanism in a Human Trachea

M. MALVÈ,^{1,2,3} A. PÉREZ DEL PALOMAR,^{1,2,3} J. L. LÓPEZ-VILLALOBOS,⁴ A. GINEL,⁴ and M. DOBLARÉ^{1,2,3}

¹Group of Structural Mechanics and Materials Modeling, Aragón Institute of Engineering Research (I3A), Universidad de Zaragoza (Spain), C/María de Luna 3, 50018 Zaragoza, Spain; ²Centro de Investigación Biomédica en Red en Bioingeniería Biomateriales y Nanomedicina (CIBER-BBN), C/María de Luna 11, 50018 Zaragoza, Spain; ³Instituto de Salud Carlos III, Madrid, Spain; and ⁴Department of Thoracic Surgery, Hospital Virgen del Rocío, Seville, Spain

(Received 7 September 2009; accepted 29 January 2010; published online 9 February 2010)

Associate Editor John H. Linehan oversaw the review of this article.

Abstract—The main physiological function of coughing is to remove from the airways the mucus and foreign particles that enter the lungs with respirable air. However, in patients with endotracheal tubes, further surgery has to be performed to improve cough effectiveness. Thus, it is necessary to analyze how this process is carried out in healthy tracheas to suggest ways to improve its efficacy in operated patients. A finite element model of a human trachea is developed and used to analyze the deformability of the tracheal walls under coughing. The geometry of the trachea is obtained from CT of a 70-year-old male patient. A fluid structure interaction approach is used to analyze the deformation of the wall when the fluid (in this case, air) flows inside the trachea. A structured hexahedral-based grid for the tracheal walls and an unstructured tetrahedral-based mesh with coincident nodes for the fluid are used to perform the simulations with the finite element-based commercial software code (ADINA R&D Inc.). Tracheal wall is modeled as an anisotropic fiber reinforced hyperelastic solid material in which the different orientation of the fibers is introduced. The implantation of an endotracheal prosthesis is simulated. Boundary conditions for breathing and coughing are applied at the inlet and at the outlet surfaces of the fluid mesh. The collapsibility of a human trachea under breathing and coughing is shown in terms of flow patterns and wall stresses. The ability of the model to reproduce the normal breathing and coughing is proved by comparing the deformed shape of the trachea with experimental results. Moreover the implantation of an endotracheal prosthesis would be related with a decrease of coughing efficiency, as clinically seen.

Keywords—Trachea, Finite element method, Fluid–solid interaction, Coughing, Fiber reinforced material.

INTRODUCTION

A cough is a sudden, often repetitive, spasmodic contraction of the thoracic cavity, resulting in violent release of air from the lungs through the tracheal airways and usually accompanied by a distinctive sound. A cough is usually initiated to clear a buildup of phlegm in the trachea; due to the high intrathoracic pressures, high expiratory flow rates are promoted (up to 12 L/s in 30–50 ms).²³ The main physiological function of coughing is to remove from the airways the mucus and foreign particles that enter the lungs during normal breathing. From a mechanical point of view, coughing has different effects on the trachea. During coughing, the tracheal cross section changes sharply,³¹ which leads to an increase in the velocity in the constriction area thus enhancing the cough efficiency.¹⁹ The ability of the trachea to deform drastically, relies in its complex anatomical structure. The trachea as a construction is a reinforced tube. Sixteen to twenty cartilaginous half-rings whose ends are connected by a soft membranous wall form the anterior tracheal wall. There is a notion that the elastic posterior wall of the trachea is necessary for the free movement of large solid pieces of food through the esophagus, which is adjacent to the posterior tracheal wall. However, the elastic behavior of this wall is also critical for ensuring an effective act of coughing which depends on the capacity of the respiratory muscles to increase intrathoracic pressures and dynamically compress the airways.²³ Thus, smooth muscle contraction and transmural pressure generate bending and tensile stresses in the cartilage and collapse it to regulate the air flow and to modulate the diameter of the airway. This mechanism is easily performed in healthy tracheas, but when there is an endotracheal prostheses the cough efficiency decreases. In patients with carcinoma or stenosis due to tracheal diseases, stents are

Address correspondence to M. Malvè, Group of Structural Mechanics and Materials Modeling, Aragón Institute of Engineering Research (I3A), Universidad de Zaragoza (Spain), C/María de Luna 3, 50018 Zaragoza, Spain. Electronic mail: mmalve@unizar.es

the primary treatment to prevent lumen collapse. These patients show difficulty to cough since the stiffness of the tracheal wall increases due to the presence of the prostheses which cannot reproduce the behavior of the muscular membrane.

Most of the developed numerical studies in the respiratory system till now have analyzed the airflow pattern using rigid walls and approximated airways geometries.^{5,20,26} Cebal and Summers⁵ developed a CFD model using a four-generations geometry. They studied the central tracheal and bronchial airways by using a virtual bronchoscopy reconstruction method. Nowak *et al.*²⁶ demonstrated a four-subunit CFD simulation method for the human tracheobronchial tree. They economized on computational effort by segmenting the first 12 generations into four generation “tranches.” Ma and Lutchen²⁰ developed a six-generations model in which flow pattern were predicted under turbulent conditions using zero-pressure outlet conditions. Only few studies are based on an accurate airway geometry coming from computed tomography (CT) or magnetic resonance (MRI).^{18,25,40,39} Moreover, these studies (both using simplified or real geometries) do not take airway deformation and fluid–solid interaction (FSI) into account.^{1,4,16,17,20,26,38} In particular, Zhang and Kleinstreuer³⁹ analyzed targeted aerosol drug deposition in a rigid triple bifurcation tracheobronchial airway model. Nithiarasu *et al.*²⁵ performed a steady-state simulation of a human tracheal model while Liu *et al.*¹⁸ analyzed the unsteady flow patterns in a patient-specific human healthy trachea during inspiration under turbulent condition.

Regarding solid mechanics, Costantino *et al.*⁶ analyzed the collapsibility of the trachea under different pressure conditions, although they did not considered the fluid itself. FSI studies in lower airway geometries were done only in the lower cartilage-free generations of the lung and were restricted to simplified models/geometries and to single bifurcations.^{11,12,13,30,36} Only the work developed by Wall and Rabczuk³⁵ analyzed the behavior of the trachea using a FSI analysis although they considered a simplified model for the composing material. Regarding the constitutive behavior of the tracheal walls, there is a large dispersion of the mechanical properties of the different tissues that composed the trachea, and only few studies have analyzed their mechanical behavior for humans.^{28,29,34,37} While some works isolated a single cartilage ring simplifying the material constitutive model as isotropic elastic,^{6,34} the studies of Rains and coworkers^{28,29} shed light in the tracheal cartilage properties analyzing the tensile stiffness of the human tracheal cartilage rings in specimens obtained at autopsy from 10 individuals who ranged in age from 17 to 81. Moreover, many of the previous works

studying the human tracheal smooth muscle dealt with its plasticity, stiffness and extensibility, and the influence of the temperature on force–velocity relationships.¹⁰ As far as the authors know, there is no numerical model that combines a realistic constitutive model of the tracheal walls in a fluid structure code that can predict accurate deformations of the trachea during coughing.

This paper mainly considers the mechanical phenomena in the trachea, which accompanies the normal breathing and cough act and ensure its efficiency. In first place, the material and boundary conditions assumptions will be described and then the results will be compared with images obtained from tracheal endoscopies. Finally, the influence of implanting a tracheal endoprosthesis on coughing efficiency will be analyzed.

MATERIALS AND METHODS

In this work, a fluid interaction analysis of a human trachea is developed, and the collapsibility of the wall under normal breathing and coughing is analyzed.

Solid Structure: Tracheal Walls

The finite element model of the human trachea was made based on a CT performed on a 70 years old healthy man. The DICOM files coming from the scan provide a clear picture of the internal (black) cavity filled with air. The detection of the outer surface and therefore the thickness of the wall was not so easy. With this aim, a nonautomatic segmentation of the CT scan was accomplished to determine the real geometry of the trachea and to distinguish between the muscle membrane and the cartilage rings. To identify the tracheal tissues, the cartilage rings could be isolated through their higher density. With help of MIMICS[®], the different material densities could be distinguished through different tones of the gray scale (i.e., high density corresponds to white color while low density corresponds to dark color). For the thickness, very slight variations along the tracheal axis were detected, and therefore we chose to simplify it as constant. An IGES file of the segmented geometry was created to construct the associated computational grid. A full hexahedral mesh of 29250 elements was made using PATRAN[®] (see Fig. 1), where the different tissues are shown in different colors. To avoid significant variations between segmented geometry and finite element model a grid independence study was performed. Finally, the average solid-grid element size was around 1 mm.

To determine the properties of the different tissues of the trachea, different experimental tests were

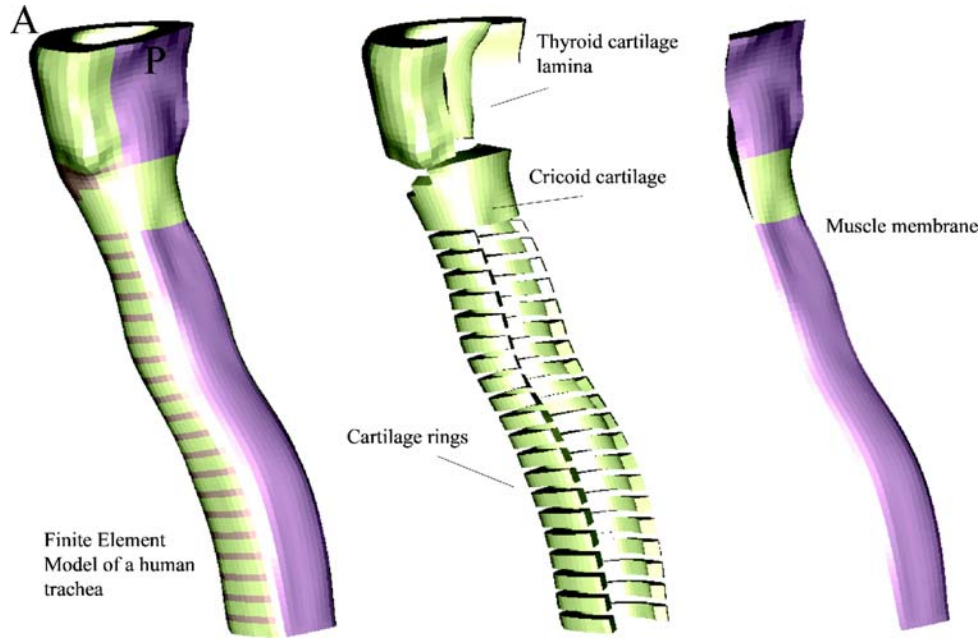


FIGURE 1. Finite element mesh of the trachea. The cartilaginous parts of the trachea are plotted separately from the muscular membrane (A denotes anterior part and P posterior part).

conducted. The goal of this paper is not the experimental characterization of the trachea, so, only a summary of the data acquisition is included. Human tracheas were obtained at the time of autopsy from two subjects (aged 79–82 years). Samples of cartilage and muscle were dissected from the tracheas for histology and mechanical analysis procedures. The histology revealed that in the cartilage rings, the collagen fibers run randomly. Therefore, an isotropic material was used to define its behavior. On the contrary, the muscular membrane presented two orthogonal families of smooth muscle cells, one running mainly longitudinally and the other transversely. Therefore, for this tissue a constitutive model that takes into account the anisotropy coming from the fiber orientation was used.

The specimens were mounted on the Instron MicroTester 5548 to perform tensile tests. For cartilage, since there is no preferential orientation, a Neo-Hookean model with strain energy density function (SEDF), $\Psi = C_1(\bar{I}_1 - 3)$, was used to fit the experimental results. Regarding the smooth muscle, and taking into account that the histology showed two orthogonal fiber families, a Holzapfel SEDF¹⁴ for two families of fibers was used,

$$\Psi = C_1(\bar{I}_1 - 3) + \frac{K_1}{2K_2} \left\{ \exp[K_2(\bar{I}_{41} - 1)^2] - 1 \right\} + \frac{K_3}{2K_4} \left\{ \exp[K_4(\bar{I}_{42} - 1)^2] - 1 \right\} + \frac{1}{D}(J - 1)^2,$$

where C_1 is the material constant related to the ground substance, $K_i > 0$ are the parameters which identify the

exponential behavior due to the presence of two families of fibers, and D is identified with the tissue incompressibility volumetric modulus. The invariants I_{ij} are defined as:

$$\begin{aligned} \bar{I}_1 &= \text{tr} \bar{\mathbf{C}}, \bar{I}_2 = \frac{1}{2}[(\text{tr} \bar{\mathbf{C}})^2 - \text{tr}(\bar{\mathbf{C}}^2)], \bar{I}_{41} = \mathbf{a}^0 \cdot \bar{\mathbf{C}} \mathbf{a}^0, \\ \bar{I}_{42} &= \mathbf{b}^0 \cdot \bar{\mathbf{C}} \mathbf{b}^0, \end{aligned} \quad (1)$$

where \mathbf{a}^0 is a unitary vector defining the orientation of the first family of fibers and \mathbf{b}^0 the direction of the second family both in the reference configuration, and $\bar{\mathbf{C}}$ is the modified right Green strain tensor defined as $\bar{\mathbf{C}} = J^{1/3} \mathbf{C}$ being $\mathbf{C} = \mathbf{F}^T \mathbf{F}$.

The longitudinal and transversal tensile behavior of the tracheal muscle was analyzed, and the parameters of the SEDF were calculated by fitting the constitutive equation of Holzapfel to the experimental results obtained in our lab (see Fig. 2). See Table 1 for a summary of the material constants used for the different tissues.

Solid Structure: “Virtual” 2D Stent

On the other hand, as mentioned in the “Introduction,” section, it has been clinically seen that patients with endoprotheses have difficulty in coughing because these stents are too stiff to allow the trachea to deform. In this study, a “virtual” 2D model of the protheses was considered. The external surface of the prothesis was introduced so that the trachea adapts its shape to the allocated stent. The deformation of the

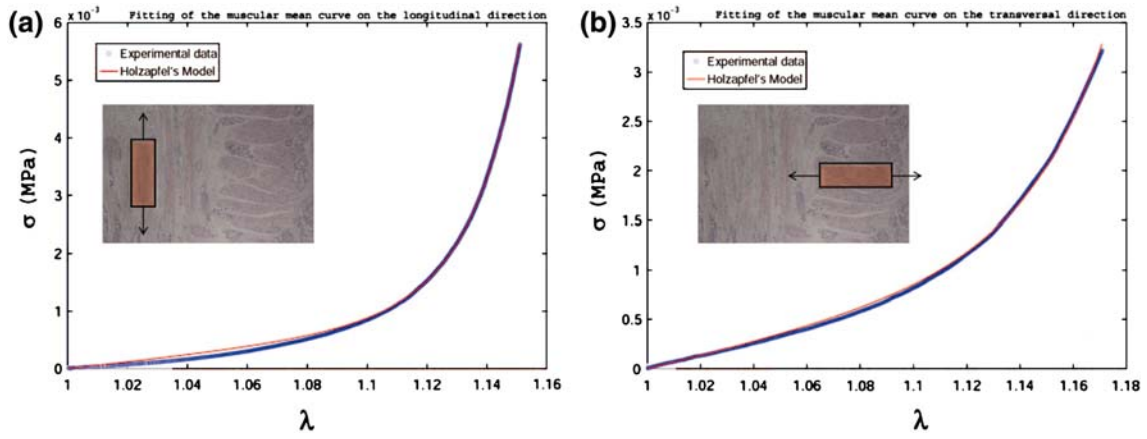


FIGURE 2. Uniaxial tests performed to tracheal muscle samples. Fitting of the Holzapfel's model to the experimental results obtained in a tensile test in (a) the longitudinal direction of the trachea and in (b) the transversal direction of the trachea.

TABLE 1. Parameters to define the constitutive models to characterize the mechanical behavior of cartilage and muscular membrane.

Material parameters	C_1 (KPa)	K_1 (KPa)	K_2	K_3 (KPa)	K_4
Cartilage	577.7	–	–	–	–
Muscular membrane	0.87	0.154	34.15	0.34	13.9

trachea due to the introduction of the 2D prostheses was performed in ABAQUS with the prostheses introduced as a silicone surface (elastic material with Young modulus $E = 1$ MPa and Poisson coefficient $\nu = 0.28$) with the real dimensions of a Dumon prostheses. It has to be noticed that the study with stent has to be considered as the first step to create a useful tool that in the future may help surgical treatment of diseased patients and evaluate physical variables that cannot be assessed *in vivo*. In Fig. 3, the equivalence of a real prostheses⁹ and the “virtual” stent is shown.

Fluid: Airway Flow

Starting from the inner tracheal wall an unstructured tetrahedral-based fluid grid was generated using the commercial software FEMAP (Siemens PLM Software). The total number of tetrahedral elements was 59581. The fluid, in this case air, was assumed Newtonian ($\rho_F = 1.205$ kg/m³, $\mu = 1.83 \times 10^{-5}$ kg/m s) and incompressible under unsteady flow conditions. Two different conditions were analyzed. First, the deformation of the trachea under normal breathing was simulated. In this case, flow was assumed laminar since the Reynolds number, based on the median tracheal diameter, was less than 2300. On the other hand, coughing involves higher flow velocities. During this process, after a larger inspiration phase, a shorter high speed expiration phase follows. In this phase,

a maximum flow rate can reach 12 L/s and air is supposed to flow out in a period of time of 0.3–0.5 s.²³ Therefore, airflow is modeled as turbulent (Reynolds number in the trachea is around 10000). A turbulence model (k - ϵ model) is then used to modify the air viscosity in order to include the turbulent effect on the flow. In particular in the Navier–Stokes equations the viscosity μ is substituted by $\mu_0 = \mu + \mu_t$ where μ_t is the turbulent viscosity that is expressed as:

$$\mu_t = \rho_F \cdot C_\mu \cdot \frac{K^2}{\epsilon}, \quad (2)$$

where $C_\mu = 0.07469$ is a constant, and, K and ϵ are called kinetic energy and rate of dissipation of the turbulence, defined as follows:

$$K = \frac{1}{2} \overline{\mathbf{v}' \cdot \mathbf{v}'}, \quad \epsilon = \frac{\mu}{\rho_F} \overline{(\nabla \mathbf{v}') \otimes (\nabla \mathbf{v}')} \quad (3)$$

where \mathbf{v}' is the fluctuating velocity. A complete description of this turbulence model is made by Oertel *et al.*²⁷

Fluid–Solid Interaction

The complete mesh (solid + fluid) was imported into the software package ADINA R&D Inc., where the FSI computations were performed. In the FSI model, the fluid domain is deformable so that the numerical approach uses the well-known Arbitrary Lagrange-Euler (ALE) formulation.^{2,3} For the solid domain, a typical Lagrangian formulation^{2,8,19} is used. Taking into account the moving reference velocity, the Navier–Stokes equation becomes:

$$\rho_F \frac{\partial \mathbf{v}_F}{\partial t} + \rho_F ((\mathbf{v}_F - \mathbf{w}) \cdot \nabla) \mathbf{v}_F - \nabla \cdot \boldsymbol{\sigma}_F = \mathbf{f}_F^B, \quad (4)$$

where the term \mathbf{w} denotes the moving mesh velocity vector, \mathbf{v}_F is the velocity vector, \mathbf{f}_F^B is the body force per unit volume, and ρ_F is the fluid density.

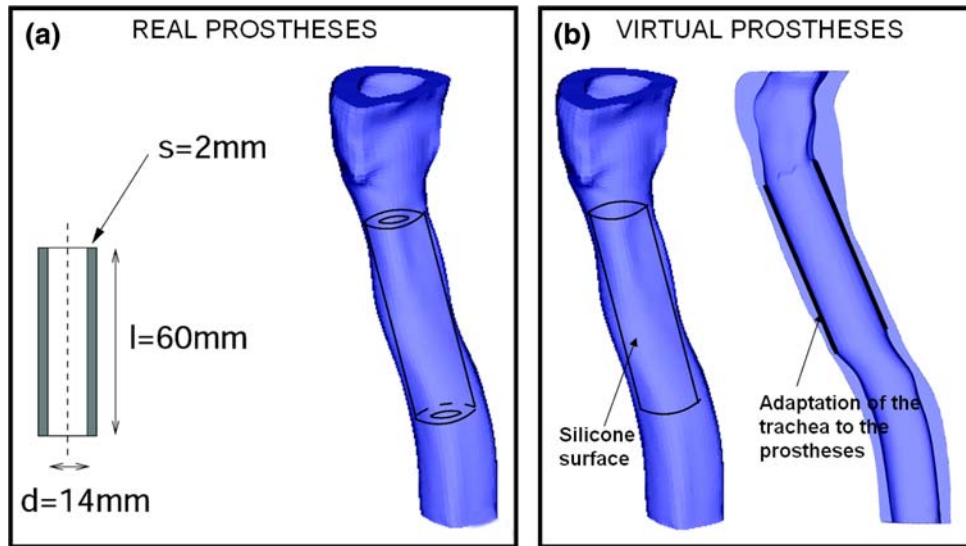


FIGURE 3. (a) Schematic representation of a Dumon prostheses and its theoretical location inside the trachea; (b) adaptation of the internal surface of the trachea to allocate the silicone surface of the prostheses.

The governing equation for the solid domain is the following momentum conservation equation:

$$\nabla \cdot \boldsymbol{\sigma}_S + \mathbf{f}_S^B = \rho_S \ddot{\mathbf{u}}_S, \quad (5)$$

where ρ_S is the solid density, $\boldsymbol{\sigma}_S$ is the solid stress tensor, \mathbf{f}_S^B is the body force per unit volume and $\ddot{\mathbf{u}}_S$ is the local acceleration of the solid. The domains described by Equations (4) and (5) are then coupled through displacement compatibility and traction equilibrium² with the following equations:

$$\mathbf{u}_S = \mathbf{u}_F \quad (x, y, z) \in \Gamma_{\text{wall}}^F \cap \Gamma_{\text{wall}}^S \quad (6)$$

$$\boldsymbol{\sigma}_S \cdot \mathbf{n}_S + \boldsymbol{\sigma}_F \cdot \mathbf{n}_F = \mathbf{0} \quad (x, y, z) \in \Gamma_{\text{wall}}^F \cap \Gamma_{\text{wall}}^S, \quad (7)$$

where Γ_{wall}^F and Γ_{wall}^S are the boundaries of the fluid and solid domains, respectively (see Fig. 4). Equation (7) is an equilibrium condition between the stresses acting in normal direction on both domain boundaries Γ_{wall}^F and Γ_{wall}^S .

The movement of the solid mesh of the trachea was restrained by fixing the top and the bottom surfaces of the solid mesh assuming that the trachea is fixed both at the thyroid cartilage and the bifurcation. Regarding the fluid mesh, the pressure and air velocity were imposed at the inlet and at the outlet surfaces for the normal breathing³⁵ and coughing²³ as can be seen in Fig. 4. The imposed velocity spatial distribution on the boundary surface Γ_{outlet}^F is parabolic³⁵ although we know that this distribution is probably more complex.²⁰ Finally, the pressure distribution was imposed as a constant on the inlet surface Γ_{inlet}^F .

RESULTS

First of all, the deformation of the trachea is shown both for normal breathing and coughing. For the validation of the overall model, *in vivo* data of the trachea is necessary. To qualitative validate the numerical results, the software MatLab[®] (The MathWorks Inc.) was used. Using this software, the variations of color-scale pixels of the available endoscopic images (see Fig. 5) were distinguished. A single cartilage ring was detected, and a red colored dotted line was projected around the tracheal wall in order to make evidence of the ring deflection. This deflection, sketched in Fig. 5 for both normal breathing and coughing, was finally compared with the computed deformation of the numerical trachea model.

In Fig. 5, the qualitative validation is presented in two rows. In the first row, the deformed shape for one ring with its membrane is shown for the maximum inspiration/expiration and compared with the mentioned endoscopic images. In the second row, the deformed shape of the same ring is depicted but in this case during coughing and also compared with images obtained from a patient during this movement. It can be seen that the shape of the numerical and the experimental deformation qualitatively follows the same trend both for normal breathing and coughing. The maximum displacement of the membrane during the inspiration phase of breathing was 1 mm, while during coughing was 4 mm.

Therefore, the ability of this FSI analysis to capture changes in tracheal cross sections that were seen in

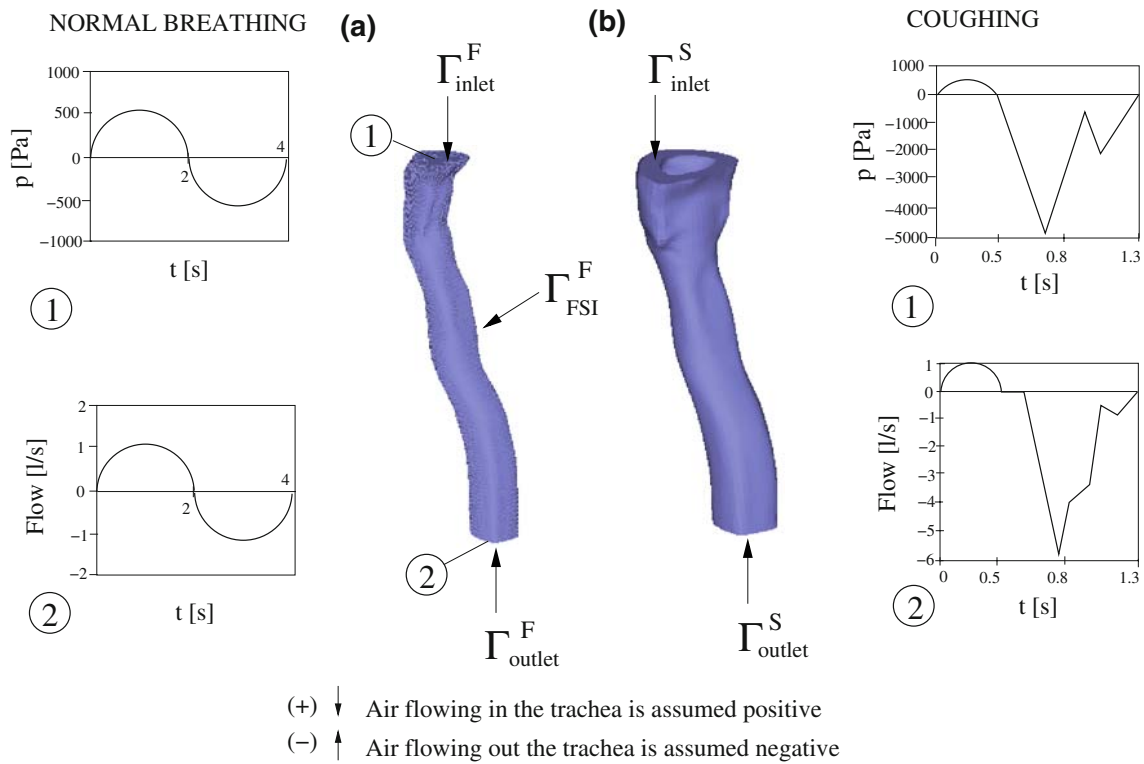


FIGURE 4. Fluid (a) and solid (b) domains. Pressure and velocity conditions imposed at the inlet (1) and outlet (2) surfaces of the fluid mesh of the trachea.

endoscopic studies was demonstrated. However, one of the most relevant aspects of this is to analyze the efficiency of a patient coughing. As mentioned before, the coughing mechanism appears when it is necessary to remove particles or mucus from the lungs, and in this regard when an endotracheal prosthesis is located, the patient partially loses this ability to cough. Here, this was analyzed by simulating the implantation of a “virtual” 2D prosthesis. Different velocity patterns were sketched in Figs. 6 and 7. To compare velocity patterns in presence and absence of the stent, the same tracheal section was analyzed for both models (Fig. 6). This section corresponded to the upper transition between the tracheal wall and the location of the prosthesis. It can be seen that the maximum fluid velocity decreased from 21 to 17.5 m/s when the presence of a stent was simulated. Moreover, the differences in the cross section can be seen for both cases, assuming the tracheal wall adapts to the internal surface of the trachea and therefore the muscular membrane does not collapse. Finally, in Fig. 7, the air velocity for the selected time points is plotted at the outflow section, in order to take into consideration the overall change in the tracheal volume due to the deformable walls. Again, the maximum fluid velocity decreases (from 20 to 17 m/s at $t = 0.78$ s and from 13 to 11 m/s at $t = 0.9$ s) confirming an overall reducing

of the velocity field during coughing in presence of this prosthesis.

DISCUSSION

We have presented an FSI analysis of a patient-specific tracheal tube under different unsteady boundary conditions. The trachea was assumed as a fiber reinforced hyperelastic solid material in which the different fiber orientations were taken into account. The properties of the tracheal wall and the fiber orientation were experimentally obtained. Besides, the influence of implanting an endotracheal prosthesis was also analyzed.

First, we simulated the normal breathing in order to evaluate the tracheal wall deformation and the flow patterns. Then, we made a comparison with the same trachea under coughing, characterized by turbulent flow. We showed that the higher air flow velocity and pressure level induced by cough caused a huge deformation of the tracheal muscular wall. Moreover, we validated the computational results of the simulation under breathing and coughing boundary conditions with *in vivo* data extracted from a tracheal endoscopy. We were able to establish a good qualitative comparison between the numerical prediction and the real

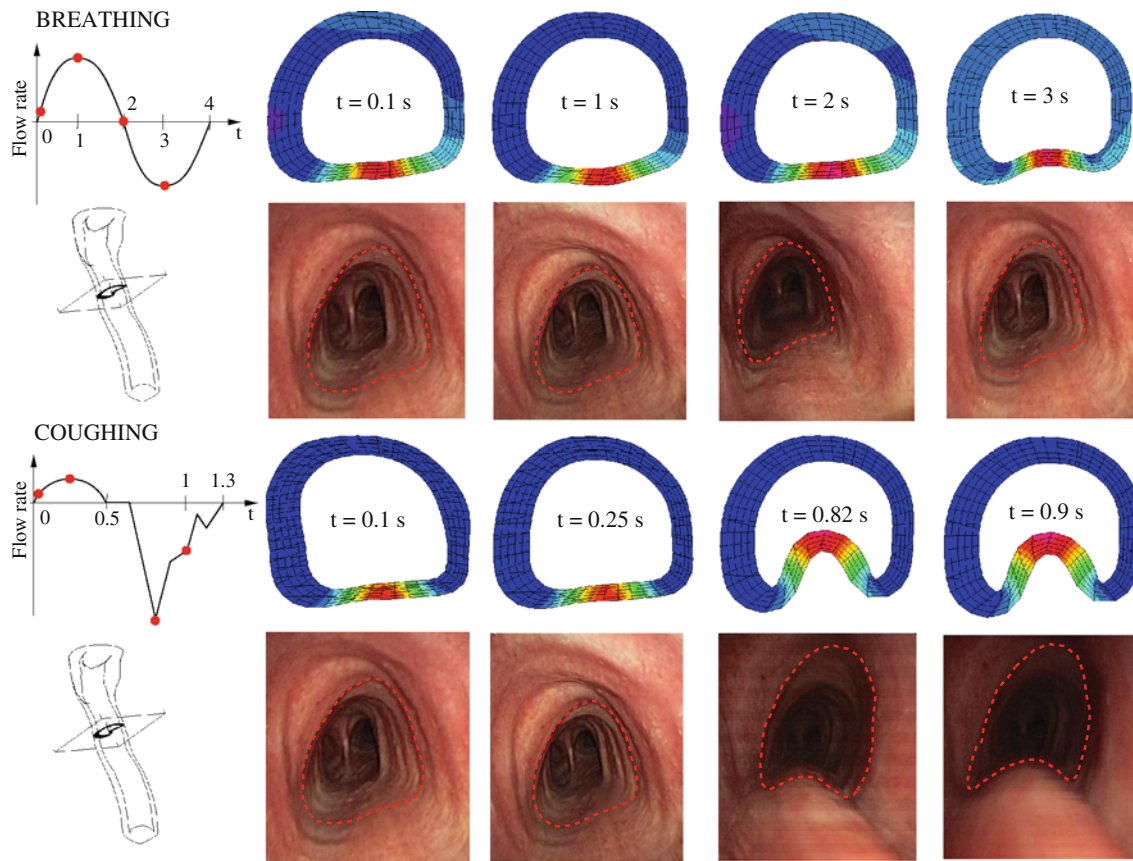


FIGURE 5. Deformed shape of a tracheal section during normal breathing (*first row*) and during coughing (*second row*). The correlation of the numerical prediction and the real deformation can be established.

muscular wall deformation. This comparison can only be qualitatively developed because it is not possible to make accurate measures of the real displacement undergone by the tracheal wall during breathing and coughing. The computed displacements (1 mm during breathing and 4 mm during coughing) lie inside the physiological range of movement of the tracheal wall. However, the deflections in the numerical model were generally larger than those seen in the *in vivo* study.

The numerical results gave an insight of how the mechanism of coughing can be captured through FSI simulations showing the muscular membrane collapsing through higher airflow velocities going out the lungs. To demonstrate a possible clinical application of this numerical model, we simulated the same human trachea in presence of an endotracheal prosthesis, modeled as a simplified 2D cylinder. In the region where the tracheal stent is located, the muscular membrane cannot collapse because the material stiffness prevents the wall prostheses from collapsing. Then the differences in the flow regime between the healthy trachea (with flexible membrane) and the trachea with a silicone stent were analyzed (see Fig. 6). It was

shown that the calculated velocity field of the air flowing out the trachea in presence of stent showed lower velocity gradients in comparison with a cough in a healthy trachea.¹⁹ This confirms the difficulty of coughing in surgically treated patients, due to an increase in the tracheal wall stiffness and a corresponding loss of muscle contraction capability.

This preliminary study shows the capability of computational models to reproduce clinical observations and pathologies in the human trachea. While it shows improvements with respect to the few studies done before, there are still many assumptions and approximations that are described. First, for this study, patient-specific boundary conditions were not available. This may not affect the numerical solution qualitatively but a quantitative effect in terms of flow velocity or wall stresses can be anticipated. In addition, the used boundary conditions did not take into account the entire respiratory system. In future works at least one bifurcation will be added to the tracheal tube and physiological conditions will be used in order to reflect the resistance of the lower/upper airways. Moreover, the stent is simulated as a molded surface so

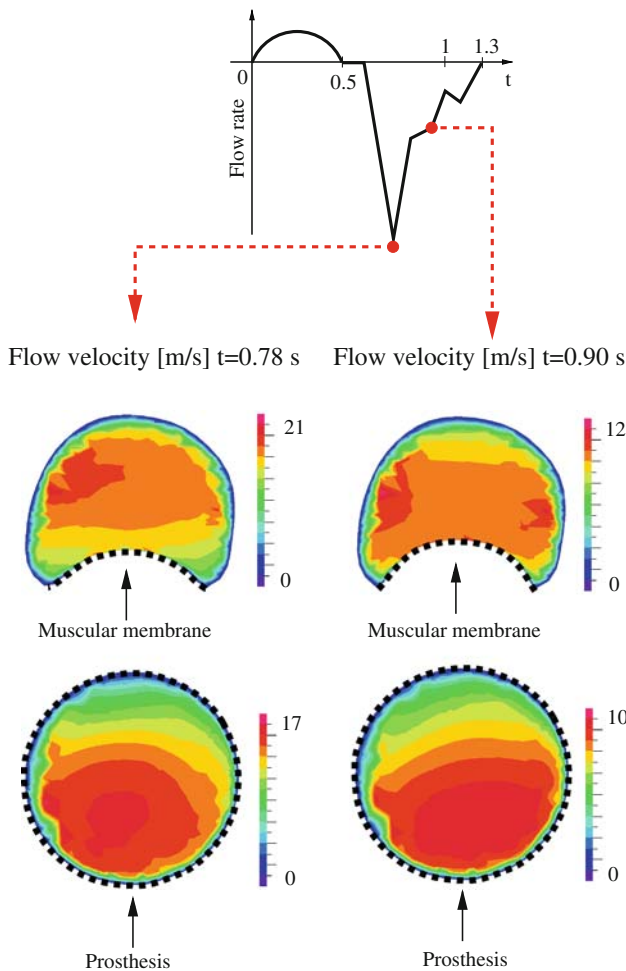


FIGURE 6. Air velocity during coughing in $t = 0.78$ s and $t = 0.9$ s. In the first row, the results for a normal (flexible) tracheal wall are presented; in the second, the prosthesis has been included.

recirculation effects near the extremities of the prosthesis due to its simplified geometry could not be analyzed. On the other hand, the implantation of the prosthesis was made by adjusting the internal surface of the trachea to the surface of the prostheses and therefore the stresses that may appear in the tracheal wall that would generate granulomas cannot be distinguished. Regarding the tracheal material properties, experimental data using samples from autopsy were obtained in our laboratory. There could be differences in tracheal properties between living specimens and the mentioned samples, but this aspect was neglected in this work, since the active response of the tracheal muscle was not considered. The influence of the active response of this muscle was not described yet, but this will be analyzed in further developments. Finally, the numerical trachea model is not surrounded by the different soft tissues present in the human neck. We modeled it as an isolated element

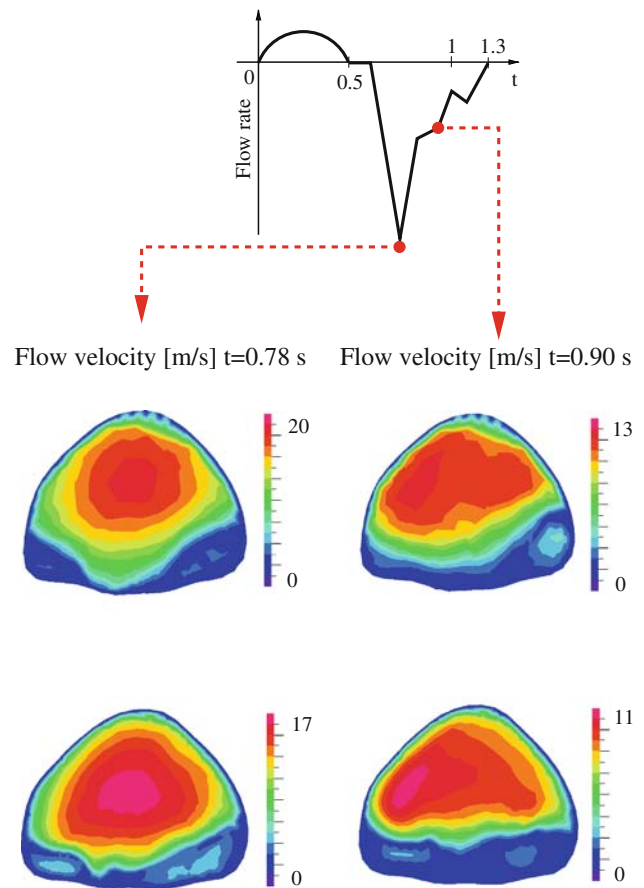


FIGURE 7. Air velocity during coughing at the outflow sections in $t = 0.78$ s and $t = 0.9$ s. In the first row, the results for a normal (flexible) tracheal wall are presented; in the second, the results for the trachea with prosthesis are shown.

which is not restricted, as it should be, in its wall displacements. This simplification can affect the wall deformation quantitatively even though it should not influence the muscular contraction and dilatation, the evaluation of which is a very important achievement of this work.

CONCLUSION

The computational model showed in this study can be used to evaluate the mechanical behavior of the trachea during breathing and coughing. Moreover, it can be considered as a first approach to analyze the influence of a tracheal stent implantation in a patient, since it is capable of giving information on the muscular wall deformation, and flow patterns coming out the trachea. An important clinical application of the computational modeling is in helping the surgeon in positioning the prostheses in order to reduce inefficiencies of the tracheal tubes and improve stenting technique.

ACKNOWLEDGMENTS

The support of the *Instituto de Salud Carlos III* through the research project PI07/90023 and the CIBER initiative is highly appreciated. The authors gratefully acknowledge the technical support of Dr. Yiguang Yan (ADINA R&D Inc.).

REFERENCES

- ¹Balashazy, I., T. Heistracher, and W. Hoffmann. Air flow and particle deposition patterns in bronchial airway bifurcations: the effect of different CFD models and bifurcation geometries. *J. Aerosol Med.* 9:287–301, 1996.
- ²Bathe, K. J., and H. Zhang. Finite element developments for general fluid flows with structural interactions, *Int. J. Numer. Methods Eng.* 60:213–232, 2004.
- ³Bathe, K. J., H. Zhang, and S. Ji. Finite element analysis of fluid flows fully coupled with structural interactions. *Comput. Struct.*, 72:1–16, 1999.
- ⁴Calay, R. K., J. Kurujareon, and A. E. Holdo. Numerical simulation of respiratory flow patterns within human lungs. *Respir. Physiol. Neurobiol.*, 130:201–221, 2002.
- ⁵Cebral J. R., and R. M. Summers. Tracheal and central bronchial aerodynamics using virtual bronchoscopy and computational fluid dynamics. *IEEE Trans. Med. Imaging* 23(8):1021–1033, 2004.
- ⁶Costantino, M. L., P. Bagnoli, G. Dini, G. B. Fiore, M. Soncini, C. Corno, F. Acocella, and R. Colombi. A numerical and experimental study of compliance and collapsibility of preterm lamb trachea. *J. Biomech.*, 37:1837–1847, 2004.
- ⁷Cullen, A. B., P. H. Cooke, S. P. Driska, M. R. Wolfson, and T. H. Shaffer. The impact of mechanical ventilation on immature airway smooth muscle: functional, structural, histological and molecular correlates. *Biol. Neonate*, 90(1):17–27, 2006.
- ⁸Donea, J., S. Giuliani, and J. P. Halleux. An arbitrary Lagrangian–Eulerian finite element method for transient dynamic fluid-structure interaction. *Comput. Methods Appl. Mech. Eng.*, 33:689–723, 1982.
- ⁹Dumon, F. A dedicated tracheobronchial stent. *Chest*, 97:328–332, 1990.
- ¹⁰Forster, C. H., W. A. Wall, and E. Ramm. Artificial added mass instabilities in sequential staggered coupling of nonlinear structures and incompressible flows. *Comput. Methods Appl. Mech. Eng.*, 196:1278–1293, 2007.
- ¹¹Hazel, A. L., and M. Heil. Three-dimensional airway reopening: the steady propagation of a semi-infinite bubble into a buckled elastic tube. *J. Fluid Mech.*, 478:47–70, 2003.
- ¹²Heil, M. Airway closure: liquid bridges in strongly buckled elastic tubes. *J. Biomech. Eng. (ASME)*, 121:487–493, 1999.
- ¹³Heil, M., and J. P. White. Airway closure: surface-tension-driven non-axisymmetric instabilities of liquid-lined elastic rings. *J. Fluid Mech.*, 462:79–109, 2002.
- ¹⁴Holzappel, G. A. *Nonlinear Solid Mechanics*. Wiley, New York, 2000.
- ¹⁵<http://www.economicexpert.com/a/Cough.htm>.
- ¹⁶Kim, C. S., and A. J. Iglesias. Deposition of inhaled particles in bifurcating airway models: I. Inspiratory deposition. *J. Aerosol Med.*, 2:1–14, 1989.
- ¹⁷Kim, C. S., A. J. Iglesias, and L. Garcia. Deposition of inhaled particles in bifurcating airway models: II. Expiratory deposition. *J. Aerosol Med.*, 2:15–27, 1989.
- ¹⁸Liu, Y., R. M. C. So, and C. H. Zhang. Modeling the bifurcation flow in a human lung airway. *J. Biomech.*, 35:465–473, 2002.
- ¹⁹Lyubimov, G. A. The physiological function of the posterior tracheal wall. *Doklady Biol. Sci.*, 380:421–423, 2001.
- ²⁰Ma, B., and K. R. Lutchen. An anatomically based hybrid computational model of the human lung and its application to low frequency oscillatory mechanics. *Ann. Biomed. Eng.*, 34(11):1691–1704, 2006.
- ²¹Maksym, G. N., L. Deng, N. J. Fairbank, C. A. Lall, and S. C. Connolly. Beneficial and harmful effects of oscillatory mechanical strain on airway smooth muscle. *Can. J. Physiol. Pharmacol.*, 83(10):913–922, 2006.
- ²²McClay, J. E. Laryngeal and tracheal stents. *eMedicine*, 2008.
- ²³McCool, D. F. Global physiology and pathophysiology of cough. *Chest*, 129:48–53, 2006.
- ²⁴Miller, T. L., Y. Zhu, A. R. Altman, K. Dysart, and T. H. Shaffer. Sequential alteration of tracheal mechanical properties in the neonatal lamb: effect of mechanical ventilation. *Pediatr. Pulmonol.*, 42:141–149, 2007.
- ²⁵Nithiarasu, P., O. Hassan, K. Morgan, N. P. Weatherill, C. Fielder, H. Whittet, P. Ebdon, and K. R. Lewis. Steady flow through a realistic human upper airway geometry. *Int. J. Numer. Methods Fluid*, 57:631–651, 2008.
- ²⁶Nowak, N., P. P. Kakade, and A. V. Annapragada. Computational fluid dynamics simulation of airflow and aerosol deposition in human lungs. *Ann. Biomed. Eng.*, 31:374–390, 2003.
- ²⁷Oertel, H. Jr. *Prandtl's Essentials of Fluid Mechanics*. New York: Springer, 2004.
- ²⁸Rains, J. K. *Mechanical Properties of Tracheal Cartilage*, MSc thesis. University of British Columbia, Vancouver, 1989.
- ²⁹Rains, J. K., J. L. Bert, C. R. Roberts, and P. D. Pare. Mechanical properties of human tracheal cartilage. *J. Appl. Physiol.*, 72:219–225, 1992.
- ³⁰Roberts, C. R., J. K. Rains, P. D. Park, D. C. Walker, B. Wiggs, and J. L. Bert. Ultrastructure and tensile properties of Human tracheal cartilage. *J. Biomech.*, 31:81–86, 1998.
- ³¹Ross, B. B., R. Gramiak, and H. Rahn. Physical dynamics of the cough mechanics. *J. Appl. Physiol.*, 8(3):264–268, 1985.
- ³²Sera, T., S. Satoh, H. Horinouchi, K. Kabayashi, and K. Tanishita. Respiratory flow in a realistic tracheostenosis model. *J. Biomech. Eng.*, 125:461–471, 2003.
- ³³Spitzer, A. R., T. H. Shaffer, and W. W. Fox. Assisted ventilation: physiologic implications and complications. In: *Fetal and Neonatal Physiology*. Philadelphia: WB Saunders Company, 1992, pp. 812–894.
- ³⁴Stephens, N. L., Cardinal, R., and B. Simmons. Mechanical properties of tracheal smooth muscle: effects of temperature. *Am. J. Physiol. Cell Physiol.*, 233:C92–C98, 1977.
- ³⁵Wall, W. A., and T. Rabczuk. Fluid-structure interaction in lower airways of CT-based lung geometries. *Int. J. Numer. Methods Fluid* 57:653–675, 2008.
- ³⁶White, J. P., and M. Heil. Three-dimensional instabilities of liquid-lined elastic tubes: a lubrication theory model. *Phys. Fluid*, 17(3):031506–031506-17, 2005.
- ³⁷Yamada, H. Mechanical properties of respiratory and digestive organs and tissues. In: *Strength of Biological*

- Materials, edited by F. Gaynor Evans. Baltimore, MD: Williams and Wilkins, 1970.
- ³⁸Yang, X. L., Y. Liu, R. M. C. So, and J. M. Yang. The effect of inlet velocity profile on the bifurcation copd airway flow. *Comput. Biol. Med.*, 36:181–194, 2006.
- ³⁹Zhang, Z., and C. Kleinstreuer. Transient airflow structures and particle transport in a sequentially branching lung airway model. *Phys. Fluid*, 14:862–880, 2002.
- ⁴⁰Zhang, Z., and R. Lessmann. Computer simulation of the flow field and particle deposition by diffusion in a 3-d human airway bifurcation. *Aerosol Sci. Technol.*, 25:338–352, 1996.
- ⁴¹Zhang, H., X. Zhang, S. Ji, Y. Guo, G. Ledezma, N. Elabbasi, and H. de Coughny. Recent development of fluid-structure interaction capabilities in the Adina system. *Comput. Struct.*, 81:1071–1085, 2003.